

Quantum Science and Technology



PAPER

Fast time-domain measurements on telecom single photons

RECEIVED
19 January 2017

REVISED
7 June 2017

ACCEPTED FOR PUBLICATION
21 June 2017

PUBLISHED
24 July 2017

Markus Allgaier¹ , Gesche Vigh¹, Vahid Ansari¹, Christof Eigner¹, Viktor Quiring¹, Raimund Ricken¹, Benjamin Brecht^{1,2} and Christine Silberhorn¹

¹ Integrated Quantum Optics, Applied Physics, University of Paderborn, D-33098 Paderborn, Germany

² Clarendon Laboratory, Department of Physics, University of Oxford, Oxford OX1 3PU, United Kingdom

E-mail: markus.allgaier@upb.de

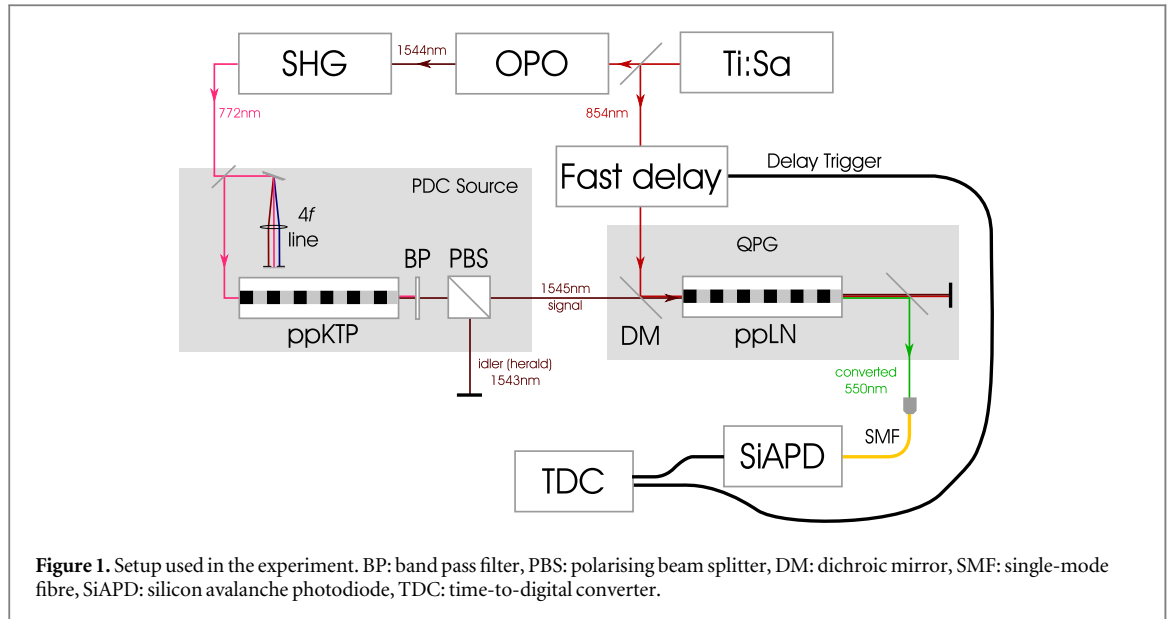
Keywords: quantum optics, time-domain, non-linear optics, ultrafast pulse characterisation

Abstract

Direct measurements on the temporal envelope of quantum light are a challenging task and not many examples are known because most classical pulse characterisation methods do not work on the single-photon level. Knowledge of both spectrum and timing can, however, give insights on properties that cannot be determined by the spectral intensity alone. While temporal measurements on single photons on timescales of tens of picoseconds are possible with superconducting photon detectors, and picosecond measurements have been performed using streak cameras, there are no commercial single-photon sensitive devices with femtosecond resolution available. While time-domain sampling using sum-frequency generation has already been exploited for such a measurement, inefficient conversion has necessitated long integration times to build the temporal profile. We demonstrate a highly efficient waveguided sum-frequency generation process in Lithium Niobate to measure the temporal envelope of single photons with femtosecond resolution with short enough acquisition time to provide a live-view of the measurement. We demonstrate the measurement technique and combine it with spectral measurements using a dispersive-fibre time-of-flight spectrometer to determine upper and lower bounds for the spectral purity of heralded single photons. The approach complements the joint spectral intensity measurements as a measure on the purity can be given without knowledge of the spectral phase.

Introduction

One key aspect to assess the quality and usability of single photons is the spectral purity [1]. An established means of measuring this quantity is through interference with a known reference pulse [2]. There is also the possibility to ascertain the photon purity in biphoton states generated through spontaneous parametric down-conversion (PDC) by measuring the joint spectral intensity. However, this works only under the assumption that no non-linear phase terms are present on both the PDC pump and phasematching function [3]. This is due to the fact that one needs the complete spectral or temporal information including phase information, which is hard to measure even though it is possible in both the spectral and the temporal domain. Complete intensity and phase characterisation of the spectrum of single photons was demonstrated by using spectral shearing interferometry [4, 5]. Homodyne detection enables the intensity and phase characterisation of the temporal envelope [6]. There is, however, also the option of combining temporal and spectral intensity information. As the time-bandwidth-product (TBP) can be extracted from intensity measurements, it can be determined with relative ease, and it was shown that the time-bandwidth-product contains information on purity [3, 7]. As spectral intensity measurements can be determined both by time-of-flight dispersive-fibre spectrometers [8] and commercially available single photon sensitive spectrometers, one only needs a means of temporal intensity characterisation. Among these are homodyne detection [9, 10], streak cameras [11, 12] and ultrafast sampling using sum-frequency generation (SFG) [13, 14]. Temporal measurements by up-conversion sampling are particularly interesting because they can in principle be highly efficient and therefore measure the temporal envelope with a short integration time. A single photon is up-converted using a sum-frequency generation with a short duration



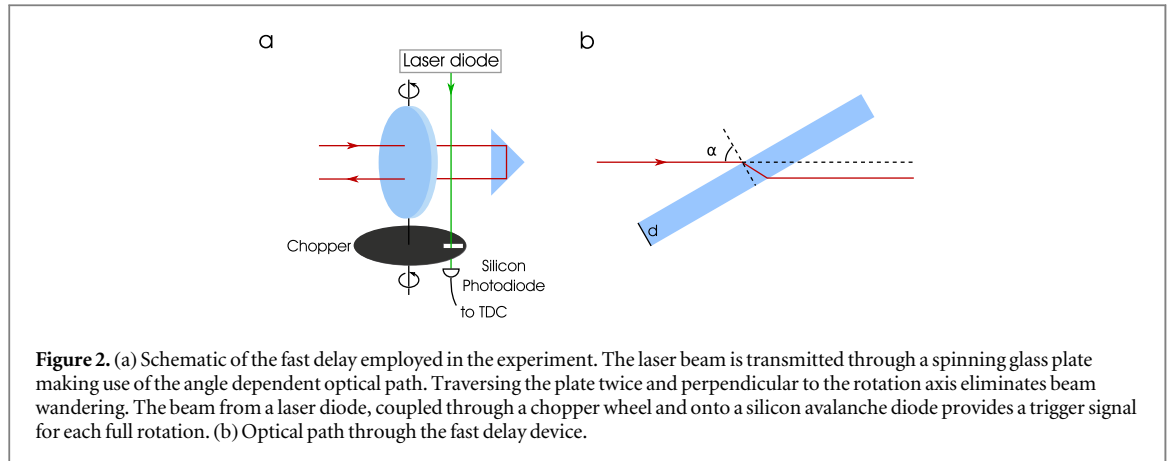
pump pulse. The short pulse has only limited overlap with the single photon and therefore the conversion efficiency depends on the relative timing between the two pulses and, most notably, on the temporal shape of the single photon. As pulse walk-off in non-linear crystals reduces the resolution of the system, existing works have used short non-linear crystals for SFG at the expense of efficiency. Carefully balanced dispersion is necessary to increase the interaction length while maintaining femtosecond resolution.

In this work we extend the method of ultrafast up-conversion sampling to long non-linear crystals with dispersion engineering to significantly improve the efficiency of the process and therefore reduce measurement time drastically. We employ the quantum pulse gate (QPG) [15, 16], a device recently introduced by our group, as a platform to perform these up-conversion measurements. This device is developed around a group-velocity matched, temporal overlap-sensitive sum-frequency generation operating with high efficiency [17]. This way we cut down the measurement times by one order of magnitude compared to [13]. In combination with a fast delay device, fast temporal envelope measurements are demonstrated. We combine time-domain measurements with spectral data to determine the purity of single photons generated by a PDC process.

Methods

The process we use to sample single photons in the time domain requires an efficient up-conversion that is sensitive to temporal overlap. The conversion process in the QPG employed here takes place in Titanium-indiffused waveguides in Lithium Niobate. In a type-II non-linear process, we mix the 1545 nm single photon input with 854 nm pump light, generating an output at 550 nm. The poling period of the 27 mm long sample is 4.4 μm . A long interaction length is achieved by matching the group velocities of the pump and the field under investigation. This is done by counteracting the material and waveguide dispersion with material birefringence. As the two pulses travel at the same speed through the waveguide, the conversion efficiency is highly dependent on the temporal overlap, which stays constant. Therefore, assuming that the pump pulse is sufficiently short in duration, the other input's temporal envelope can be recovered as a function of the delay between the two pulses. This is similar to the method described in [13], where a short crystal was used. Conversion efficiency scales with both interaction length and pump pulse energy, and as there are physical limitations for increasing the latter, increasing the interaction length is the only way to increase the efficiency. The group-velocity matching ensures that there is no pulse walk-off in first order regardless of the crystal length and makes the significantly larger conversion efficiency possible. In addition, for the comparably small spectral bandwidths considered in this work, effects of higher-order dispersion can be neglected.

We show our experimental setup in figure 1. We characterise light from a PDC source similar to the one described in [18]. It is a 8 mm long KTP crystal with Rubidium exchanged waveguides, poled over a length of 6 mm with a poling period of 117 μm . The source is pumped with 772.5 nm light produced by a cascade of a Coherent Chameleon II Ti:Sapphire laser with a repetition rate of 80.165 MHz, APE Compact optical parametric oscillator (OPO), and a periodically poled bulk Lithium Niobate crystal for second-harmonic generation (SHG). The light has a full-width-at-half-maximum (FWHM) bandwidth of 3 nm and can be spectrally filtered by means of a folded 4f line with a grating and a variable slit in the focal plane of a lens.



The photons from the type-II PDC process are split up by a polarising beam splitter and coupled into single-mode fibres and detected using superconducting nanowire single photon detectors (SNSPDs), achieving a heralding efficiency of $28.1 \pm 0.1\%$. This number is already corrected for the detector efficiency of 90%. The signal photon is then coupled through the QPG where it interacts with the fundamental Ti:Sapphire beam. The light coming out of the QPG is spectrally separated using dichroic mirrors, coupled into fibres and detected using a SNSPD for the unconverted light and a silicon avalanche photodiode (SiAPD) for the converted green light.

However, the highly efficient SFG process is only the first of two aspects that facilitates short measurement times. A second necessity for a quick or even ‘live-view’-like measurement on sub-second timescales is a means of changing the delay between the two fields in a quick, repeatable and controlled way. We identified three ways of managing these requirements: acousto-optic pulse shapers, fast linear piezo stages and rotating glass plate delays. Acousto-optic pulse shapers are expensive and have limited wavelength range. Fast linear piezo stages exist, but they are also expensive and the oscillating movement at rates of several Hertz requires significant engineering efforts for the optics’ mounts on top of the stage. The last technique, using a rotating glass plate as a delay, is known from applications such as optical auto-correlation [19] and terahertz imaging [20] as depicted in figure 2.

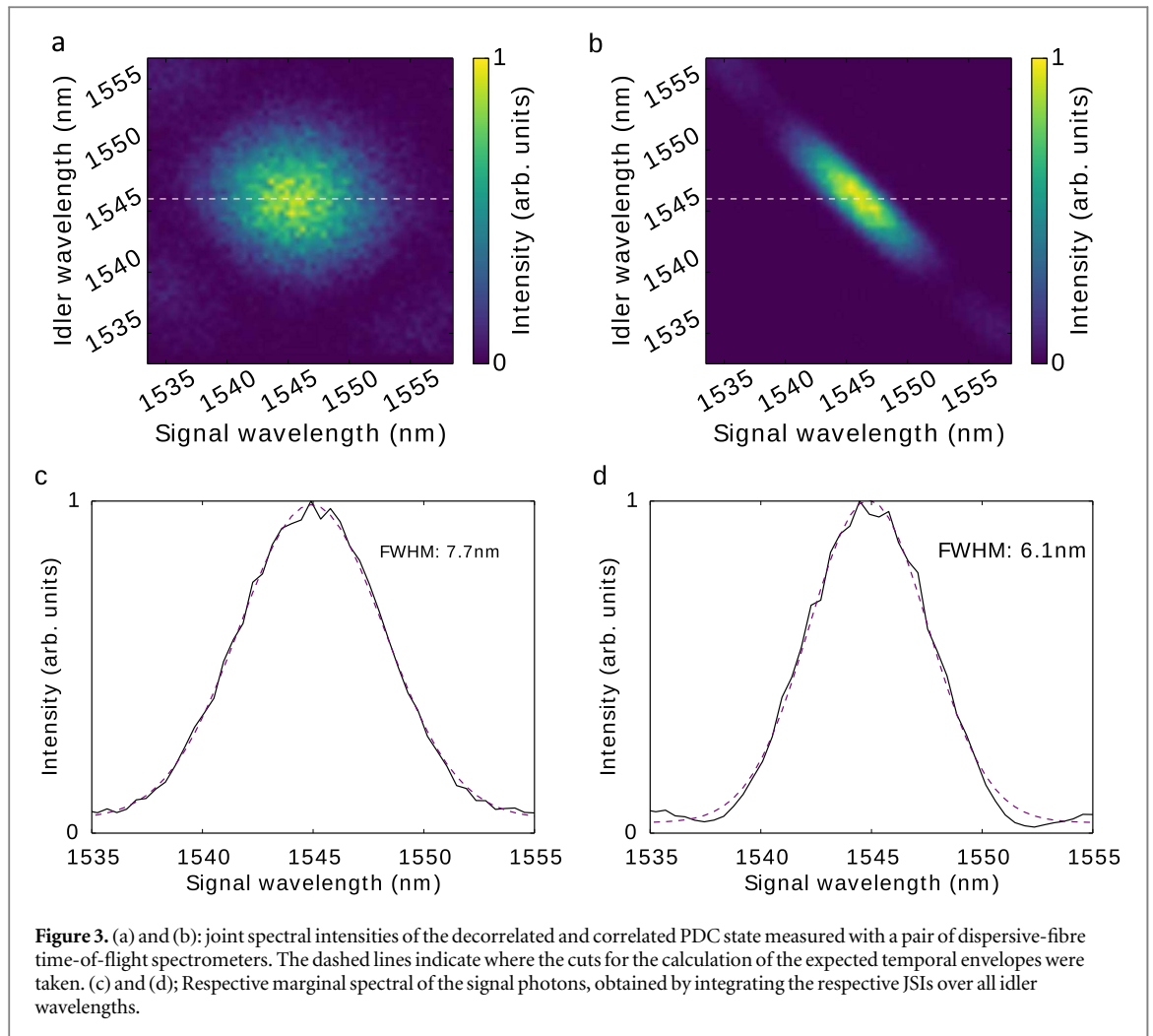
A polished glass plate of 12 mm thickness is mounted in a 3D-printed frame. The frame, supported by ball bearings, is then driven by a DC motor to rotate at 50 Hz. The frame also holds a chopper plate that opens the beam path of a green laser beam only once per rotation. The incident light on a SiAPD gives rise to the signal used as a trigger and recorded by the time-to-digital converter (TDC). The pump laser beam for the SFG process passes the plate twice as shown in figure 2(b). The optical path d_o through the plate is

$$d_o(\alpha) = \frac{d}{\cos\left(\arcsin\frac{\sin\alpha}{n}\right)}, \quad (1)$$

where α is the incidence angle of the beam on the plate and n is the glass plates refractive index. The plate is made from silica glass with a refractive index of 1.45. When the incidence angle is not zero there is an additional optical path introduced, resulting in the delay

$$\Delta\tau_{\max} = 2 \cdot \frac{d_o(\alpha_C) - d}{c_0}. \quad (2)$$

As there are reflections on the glass surface, the transmitted power depends on the angle. The incident light is in parallel polarisation and we adjust an additional manual delay stage so that the sampling of the waveform takes place when the incidence angle on the glass plate is between perpendicular incidence and the brewster angle. This guarantees an almost constant power level transmitted through the device. Within this bound the delay range of the device is 12.8 ps, which is also the longest waveform that can therefore be sampled by our setup. However, the longest pulses our experiment can produce are significantly shorter than the sampled interval. As the device goes through this delay range four times during one rotation, the waveforms are sampled 200 times per second. From the laser source’s repetition rate and the delay device’s rotation speed we calculate that a waveform of this maximum length of 12.8 ps is sampled with 1000 points, meaning that the distance between two data points in the recovered waveform is 12.8 fs. The main source of error from this delay device is the fluctuation of the rotation speed. This was assessed by tracking the delay trigger signal frequency from the green laser on a oscilloscope. We then extracted the steepest slope of the curve and calculated to the shift in rotation period. We estimate that the error of the temporal duration of the measured waveform introduced by

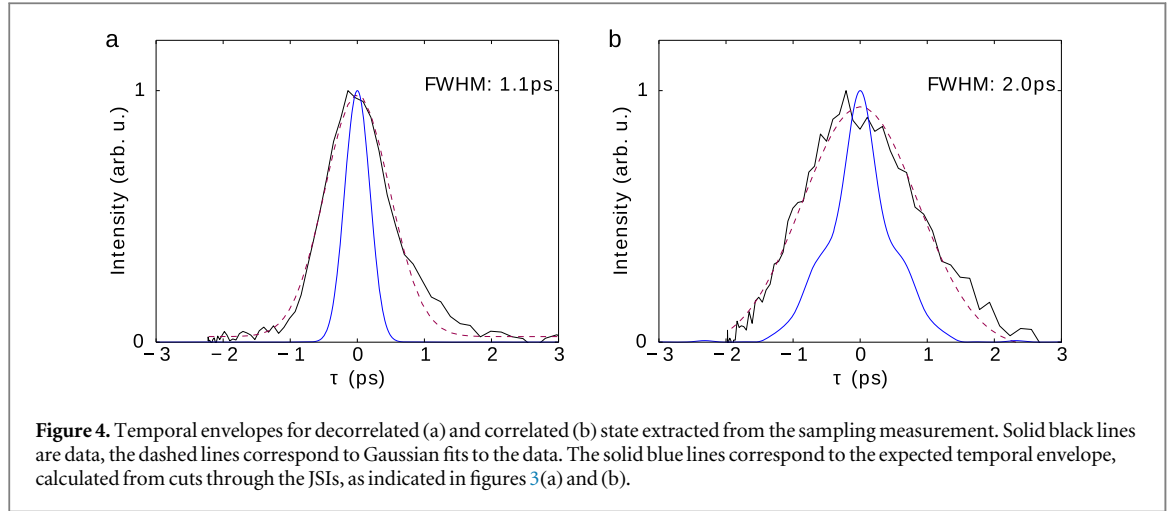


the delay is at most 70 fs. In addition, the pump pulse is stretched by 4 fs to 5.5 fs due to dispersion in the glass plate. We note that this contribution is negligible in our setup. The dominating uncertainty in the measurement is the pump pulse duration of 230 fs. There may be additional contributions such as uneven movement and vibration of the fast delay, or chirp of the sampling pulse. The practical resolution of the method was estimated by performing a measurement on a known reference generated by the optical parametric oscillator. The reference pulse has a pulse duration of 350 fs, characterised using an optical autocorrelator. By doing so a measurement uncertainty of 300 fs was ascertained. As the pump pulse duration as a source of measurement uncertainty is known, we can deconvolve the measurement result and are left with a uncertainty of 200 fs.

The rotational delay trigger signal as well as the single photon detector counts are recorded using an AIT TTM8000 TDC. We recover the single photon waveform in the arrival time histogram of the single-photon clicks relative to the rotation trigger signal, where we calculate the corresponding delay to the angle of the delay device.

Results

In the experiment we measure two different states from the PDC source. By varying the PDC pump bandwidth, we can produce both correlated and decorrelated photon pair states. These are characterised spectrally using a pair of dispersive-fibre time-of-flight spectrometers [8]. The resulting joint spectral intensities are displayed in figure 3. The decorrelated state is produced with a pump bandwidth of 3.09 nm, the correlated one with a 0.78 nm bandwidth pump. This is the smallest pump bandwidth possible with the current setup. The produced correlated state is therefore also the one with the longest pulse duration that can be produced with this experimental apparatus. Schmidt decomposition of the measured JSIs yields cooperativity numbers of $K = 1.08$ and $K = 2.10$ for correlated and decorrelated state, respectively. This implies that there is some slight correlation remaining; this is due to the fact that the phasematching angle is not perfectly perpendicular to the pump function in the JSI [21]. From the JSIs we can extract the spectral bandwidths of the PDC signal photons by



extracting the marginal spectra to obtain the FWHM bandwidth. It is $\Delta\lambda = 7.7 \text{ nm} \pm 0.1 \text{ nm}$ or $\Delta\nu = 966 \text{ GHz}$ for the decorrelated PDC state and $\Delta\lambda = 6.1 \pm 0.1 \text{ nm}$ or $\Delta\nu = 766 \text{ GHz}$ for the correlated one.

These states are also characterised with our sampling method. To obtain the temporal envelopes, the background arising from Raman scattering of the pump beam is fit and subtracted. This is possible as the noise floor has a predictable dependence on the delay devices' angle in comparison to the observed converted light. In the peak of the measured converted light we observe a signal-to-noise ratio of 10. The background-subtracted temporal envelopes are displayed in figure 4 together with the expected temporal envelopes. The expected temporal envelopes were extracted from the JSI as the Fourier transform of the conditioned marginal spectrum, i.e. by taking a cut through the JSI along the lines indicated in figure 3, and assuming a flat spectral phase (compare [3]). Only in the case of perfect decorrelation this cut is equal to the complete marginal spectrum.

The standard deviation of the Gaussian fits correspond to a pulse duration of $\Delta\tau = 1.1 \pm 0.2 \text{ ps}$ for the decorrelated state and $\Delta\tau = 2.0 \pm 0.2 \text{ ps}$ for the correlated one. We next calculate the time-bandwidth product (TBP), which is defined as

$$\text{TBP} = \Delta\tau\Delta\nu, \quad (3)$$

where $\Delta\tau$ and $\Delta\nu$ are the intensity FWHM of the temporal and spectral envelopes, respectively. The time-bandwidth product is $\text{TBP} = 1.1 \pm 0.2$ and $\text{TBP} = 1.5 \pm 0.2$ for the decorrelated and correlated state, respectively. From the measured marginals and the calculated theoretical temporal envelopes we expect $\text{TBP} = 0.57$ and $\text{TBP} = 1.1$ for the decorrelated and correlated state, respectively. This discrepancy implies that a flat phase on the JSI cannot be assumed. The source of additional higher-order phase terms cannot be deduced from the results; it could lie both in front and after the PDC source. Most notably, the results show that the validity of the flat-phase-assumption is impossible to verify with spectral intensity measurements only.

With our setup, we completed the measurement of each temporal envelope in 150 s, sampling an interval of 12.8 ps. In comparison, a 4 ps long window was sampled in 24 min in [13]. Therefore, our setup completed the same task 9.6 times quicker while sampling an interval more than three times longer. Reducing the thickness of the glass plate and therefore the sampled interval, would further decrease the measurement time by a factor of 3. At this point, it is noteworthy that due to the overlap-sensitive nature of the frequency conversion process there is a trade-off between conversion efficiency and measurement accuracy, which is mainly limited by the pump pulse duration.

Discussion

While we measure a decorrelated joint spectral intensity, which by itself is a weak indication for pure photons, the corresponding TBPs are higher than the Fourier limit. From the increased TBP, it is clear that the spectral phase is not flat and there are chirps on the photons. Such chirps could be introduced both after the generation process, or before as a chirp on the PDC pump [22]. Both do not show up in the JSI. While a separable chirp introduced after the generation leaves the photon's purity unchanged, a pump chirp has an influence on the multimodeness and of the single photon created [3]. Measuring the temporal envelope together with the spectrum provides additional information about the purity over merely taking a JSI.

As the TBP alone does not contain information about phase and pulse shape, and especially not about the source of chirps, we cannot directly calculate back from it. If the TBP is higher than the Fourier limit, it is not possible to reconstruct if there are non-linear spectral phases present or how multimode the state has gotten. To

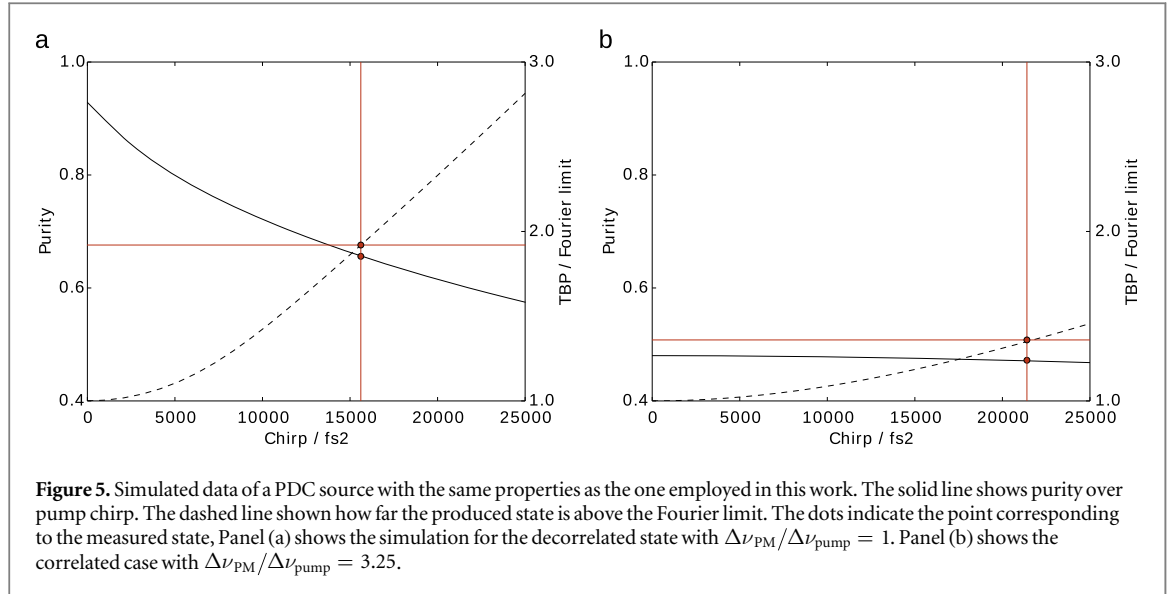


Figure 5. Simulated data of a PDC source with the same properties as the one employed in this work. The solid line shows purity over pump chirp. The dashed line shows how far the produced state is above the Fourier limit. The dots indicate the point corresponding to the measured state, Panel (a) shows the simulation for the decorrelated state with $\Delta\nu_{PM}/\Delta\nu_{pump} = 1$. Panel (b) shows the correlated case with $\Delta\nu_{PM}/\Delta\nu_{pump} = 3.25$.

get the exact purity, one would need to calculate a ‘conditioned TBP’ as shown in [3]; it is calculated from conditioned bandwidths, i.e. the temporal duration of the signal when the arrival time of the idler is fixed, and spectral bandwidth with fixed idler frequency. To do so, one needs either both joint spectral and joint temporal intensity or a means of both spectral and temporal filtering. However, if the state is known, one can calculate both the purity and the TBP. By simulating the PDC source numerically we can carry out this calculation. By attributing any occurring non-linear spectral phases to the PDC pump we obtain a lower bound on the purity.

On the other hand, by performing a Schmidt decomposition on the measured joint spectral intensities and assuming a flat spectral phase, an upper bound for the purity is extracted:

$$P = \text{tr}(\rho^2) = \frac{1}{K}, \quad (4)$$

where ρ is the density matrix of the state and K is the cooperativity number. For the decorrelated state, the Schmidt number K is 1.08 and for the correlated one it is 2.10, yielding purities of 0.93 and 0.48 respectively.

From the measured JSIs, we can infer the bandwidths of phasematching and pump. By simulating the source with the measured parameters, numerically we can calculate TBP and purity in dependence of linear pump chirp. For the calculations, we first simulate the joint spectral amplitude (JSA) using a double-Gaussian approximation, where a linear chirp can be applied to the pump function. The ‘angle’ of the phasematching function in respect to the contour plot axes of the signal and idler frequencies, which strongly impacts spectral-temporal correlations, is taken from the measured data. Moreover, $\Delta\nu_{PM}$ and $\Delta\nu_{pump}$, the phasematching and pump bandwidths, respectively, match the ones measured in the experiment. The JSA is calculated from the JSA and reproduces the experimentally measured one. Now we extract the purity according to equation (4) from the JSA by performing a Schmidt decomposition. Since we do this using the JSA instead of the JSI, this number contains the contribution from the chirp. Then the TBP is calculated. From the JSA, we calculate the marginal spectrum of one of the photons. By cutting through the JSA and performing a Fourier transform, we calculate the temporal envelope. Further details on the numerical calculations are available in [3, 17].

The result is depicted in figure 5 for both the decorrelated state and correlated state. In the experiment, we measure a TBP that is 1.92 times the Fourier limit for the decorrelated and 1.36 times higher for the correlated case. From that, we can infer pump chirp and purity from the curves plotted. The corresponding pump chirp for the two cases are 15616 fs² and 21400 fs², respectively, where the chirp parameter C is defined via the quadratic phase term as $\exp(i\omega^2 C)$. These group delay dispersion values correspond to 0.81 m or 1.11 m of fused silica glass, respectively. The purity of the states are 0.656 and 0.472. Interestingly, the purity is almost not reduced by the effect of the pump chirp in the correlated case, the decorrelated state is affected much more drastically. These numbers should only be interpreted as an estimate: the numerical modelling needs to be very accurate and any deviation in terms of correlations in the JSI would impact these numbers significantly. For a precise measurement without the need of further numerical modelling, one would also need a conditioned marginal temporal intensity, or a JTI measurement, as pointed out in [3]. This would mean duplicating the entire QPG setup for the second PDC photon. The fact that we obtain a different pump chirp for the two states is an indication that there are either higher-order non-linear spectral phase contributions or that the increase of the measured TBP is partially due to separable chirps introduced after the PDC process. Therefore, we conclude that the actual purity is between the upper and lower bounds we ascertained. It is noteworthy that there is a relatively simple

way of optimising a PDC source for maximum singlemodeness. By measuring the unheralded second-order correlation function $g^{(2)}(0)$, one gets an exact measure of the multimodeness of the state, containing all contributions from PDC pump chirps [23]. This optimisation has been employed to build PDC sources for highly pure heralded single photons [18]. However, it gives only information about the spectral correlations at the moment of generation. Even if the source has been optimised using marginal second-order correlation function as a measure of multimodeness of the source, the combination of spectral and temporal intensity measurements can aid to identify sources of additional higher-order phase contributions that occur after the PDC source.

Conclusions

We demonstrated a setup for measuring the temporal intensity distribution of single photons from a PDC source with high efficiency. Such time-domain sampling using a fast delay and long SFG crystals can, if the setup is duplicated for the second PDC photon, also drastically increase measurement speed of the joint temporal intensity measurement as in [13]. While the authors in [13] reported measurement times in the range of 30 minutes, our setup can achieve measurement times of less than three minutes. With the combination of joint spectral intensity and temporal intensity measurement, we were able to identify single photon chirps and with the help of numerical modelling establish concrete upper and lower bounds for the single photon's spectral purity. If one were to combine two of the devices, one for each PDC photon, the joint temporal intensity could be measured. This completes the characterisation of the spectral-temporal structure and correlations of photon pair states. With knowledge of joint spectral and temporal intensities, the phase information could also be reconstructed.

Acknowledgements

The authors thank Bastian Reitemeier, Regina Kruse and John Donohue for genuinely useful contributions. This work was funded by the Deutsche Forschungsgemeinschaft via SFB TRR142, grant number TRR142/1 and via the Gottfried Wilhelm Leibniz-Preis, grant number SII 115/3-1.

ORCID

Markus Allgaier  <https://orcid.org/0000-0002-2179-6250>

References

- [1] Migdall A, Polyakov S, Fan J and Bienfang J 2013 Single-photon generation and detection *Experimental Methods in the Physical Sciences* 1st edn, ed Migdall *et al* (Amsterdam; Boston, MA: Academic Press) 45 1–562
- [2] Cassemiro K N, Laiho K and Silberhorn C 2010 Accessing the purity of a single photon by the width of the Hong-Ou-Mandel interference *New J. Phys.* **12** 113052
- [3] Brecht B and Silberhorn C 2013 Characterizing entanglement in pulsed parametric down-conversion using chronocyclic Wigner functions *Phys. Rev. A* **87** 053810
- [4] Fittinghoff D N, Walmsley I A, Bowie J L, Sweetser J N, Jennings R T, Krumbügel M A, DeLong K W and Trebino R 1996 Measurement of the intensity and phase of ultraweak, ultrashort laser pulses *Opt. Lett.* **21** 884–6
- [5] Davis A O, Karpinski M and Smith B J 2016 Single-photon temporal wave function measurement via electro-optic spectral shearing interferometry *In 2016 Conf. on Lasers and Electro-Optics, paper FTu4C.6*
- [6] Qin Z, Prasad A S, Brannan T, MacRae A, Lezama A and Lvovsky A 2015 Complete temporal characterization of a single photon *Light: Science & Applications* **4** e298
- [7] URen A B, Jeronimo-Moreno Y and Garcia-Gracia H 2007 Generation of Fourier-transform-limited heralded single photons *Phys. Rev. A* **75** 023810
- [8] Avenhaus M, Eckstein A, Mosley P J and Silberhorn C 2009 Fiber-assisted single-photon spectrograph *Opt. Lett.* **34** 2873–5
- [9] Smithey D T, Beck M, Raymer M G and Faridani A 1993 Measurement of the Wigner distribution and the density matrix of a light mode using optical homodyne tomography: application to squeezed states and the vacuum *Phys. Rev. Lett.* **70** 1244–7
- [10] Anderson M E, Munroe M J, Leonhardt U, Boggavarapu D, McAlister D F and Raymer M G 1996 Ultrafast balanced-homodyne chronocyclic spectrometer *Proc. of Generation, Amplification, and Measurement of Ultrafast Laser Pulses III, SPIE* **2701** 142–51
- [11] Amann M, Veit F, Bayer M, Gies C, Jahnke F, Reitzenstein S, Höfling S, Worschech L and Forchel A 2010 Ultrafast tracking of second-order photon correlations in the emission of quantum-dot microresonator lasers *Phys. Rev. B* **81** 165314
- [12] Wiersig J *et al* 2009 Direct observation of correlations between individual photon emission events of a microcavity laser *Nature* **460** 245–9
- [13] Kuzucu O, Wong F N C, Kurimura S and Tovstonog S 2008 Joint temporal density measurements for two-photon state characterization *Phys. Rev. Lett.* **101** 153602
- [14] Kuzucu O, Wong F N C, Kurimura S and Tovstonog S 2009 Two-photon joint temporal density measurements via ultrafast single-photon upconversion *In 2009 Conf. on Lasers and Electro-Optics and 2009 Conf. on Quantum electronics and Laser Science IThJ6*

- [15] Eckstein A, Brecht B and Silberhorn C 2011 A quantum pulse gate based on spectrally engineered sum frequency generation *Opt. Express* **19** 13770–8
- [16] Brecht B, Eckstein A, Ricken R, Quiring V, Suche H, Sansoni L and Silberhorn C 2014 Demonstration of coherent time-frequency schmidt mode selection using dispersion-engineered frequency conversion *Phys. Rev. A* **90** 030302
- [17] Allgaier M, Ansari V, Sansoni L, Ricken R, Quiring V, Brecht B, Harder G and Silberhorn C 2017 Highly efficient frequency conversion with bandwidth compression of quantum light *Nature Commun.* **8** 14288
- [18] Harder G, Ansari V, Brecht B, Dirmeier T, Marquardt C and Silberhorn C 2013 An optimized photon pair source for quantum circuits *Opt. Express* **21** 13975–85
- [19] Boggy R D, Johnson R H, Eggleston J M and Schulthess C W 1983 Rapid scanning autocorrelation detector US4406542 A
- [20] Probst T, Rehn A, Busch S F, Chatterjee S, Koch M and Scheller M 2014 Cost-efficient delay generator for fast terahertz imaging *Opt. Lett.* **39** 4863–6
- [21] Eckstein A 2012 Mastering quantum light pulses with nonlinear waveguide interactions, Kontrolle über Quantenlichtpulse durch nichtlineare Interaktion in Wellenleitern *PhD Thesis* Friedrich-Alexander-Universität at Erlangen-Nürnberg
- [22] Sanchez-Lozano X, URen A B and Lucio J L 2012 On the relationship between pump chirp and single-photon chirp in spontaneous parametric downconversion *J. Opt.* **14** 015202
- [23] Christ A, Laiho K, Eckstein A, Cassemiro K N and Silberhorn C 2011 Probing multimode squeezing with correlation functions *New J. Phys.* **13** 033027